

VIGIL: Tackling Hallucination Detection in Image Recontextualization

Joanna Wojciechowicz*

255747@student.pwr.edu.pl

Wrocław University of Science and
Technology
Wrocław, Poland

Justyna Baczyńska*

268758@student.pwr.edu.pl

Wrocław University of Science and
Technology
Wrocław, Poland

Maria Łubniewska*

268845@student.pwr.edu.pl

Wrocław University of Science and
Technology
Wrocław, Poland

Jakub Antczak*

268745@student.pwr.edu.pl

Wrocław University of Science and
Technology
Wrocław, Poland

Wojciech Kozłowski

wojciech.kozlowski@pwr.edu.pl

Wrocław University of Science and
Technology
Wrocław, Poland

Wojciech Gromski*

268725@student.pwr.edu.pl

Wrocław University of Science and
Technology
Wrocław, Poland

Maciej Zięba

maciej.zieba@pwr.edu.pl

Wrocław University of Science and
Technology, Tooploox
Wrocław, Poland

Abstract

We introduce VIGIL (Visual Inconsistency & Generative In-context Lucidity), the first benchmark dataset and framework providing a fine-grained categorization of hallucinations in the multimodal image recontextualization task for large multimodal models (LMMs). While existing research often treats hallucinations as a uniform issue, our work addresses a significant gap in multimodal evaluation by decomposing these errors into five categories: pasted object hallucinations, background hallucinations, object omission, positional & logical inconsistencies, and physical law violations. To address these complexities, we propose a multi-stage detection pipeline. Our architecture processes recontextualized images through a series of specialized steps targeting object-level fidelity, background consistency, and omission detection, leveraging a coordinated ensemble of open-source models, whose effectiveness is demonstrated through extensive experimental evaluations. Our approach enables a deeper understanding of where the models fail with an explanation; thus, we fill a gap in the field, as no prior methods offer such categorization and decomposition for this task. To promote transparency and further exploration, we openly release VIGIL, along with the detection pipeline and benchmark code, through our GitHub repository: <https://github.com/mlubneuskaya/vigil> and Data repository: <https://huggingface.co/datasets/joannaww/VIGIL>.

CCS Concepts

• General and reference → Evaluation; • Computing methodologies → Scene understanding; *Visual inspection*.

Keywords

Hallucination Detection, Image Recontextualization, Benchmark Dataset, Vision Language Models (VLM), Evaluation Metrics, Open Source, Reproducibility

*These authors contribute equally to this work.

1 Introduction

The field of conditional image generation has seen transformative growth, primarily driven by two core paradigms: Text-to-Image (T2I) synthesis, which generates imagery from scratch based on textual descriptions (e.g., Flux.1 [11], DALL-E 3 [20]), and image recontextualization, where models synthesize new scenes by blending text with specific visual subjects from reference images. State-of-the-art multimodal systems, such as Gemini 3 Pro [4], GPT-5.2, and the Qwen3-VL series [19], have pushed the boundaries of visual reasoning, enabling complex subject-driven generation with unprecedented realism. Despite these advancements, even the most capable models are frequently plagued by hallucinations—defined as visual artifacts, identity shifts, or semantic inconsistencies that lack support from the input prompts or reference images. These hallucinations are highly undesirable, as they undermine the reliability of AI systems in high-stakes industries like automated advertising or digital content creation, where maintaining the visual integrity and specific attributes of a reference product is non-negotiable.

Current research on hallucination detection has matured significantly within the T2I domain, largely focusing on the alignment between text prompts and generated pixels. While some recent methods have extended these evaluations to multimodal inputs (text + images), they typically provide coarse-grained metrics—simple numerical scores that lack interpretability. These “black-box” approaches often fail to provide descriptive feedback or distinguish between specific types of errors, such as identity distortion versus environmental mismatch. This lack of a standardized, fine-grained evaluation framework hinders the diagnostic analysis required to bridge the gap between research and production-ready applications.

To fill this gap, we introduce a systematic evaluation framework and benchmark dataset specifically designed for hallucination assessment in multimodal recontextualization. Our proposed pipeline leverages state-of-the-art models—including SAM 3 [3], DINO v3 [24], and Qwen3-VL [19] to move beyond binary scores

toward human-interpretable, descriptive feedback. We validate our approach on a newly curated dataset generated with Gemini 2.5 Flash Image, featuring high-quality manual annotations that capture the nuanced ways in which modern generative models fail.

Our primary contributions are as follows:

- We present a systematic dataset of 1269 samples generated via Gemini 2.5 Flash Image. This benchmark includes manual annotations across five distinct categories of hallucinations, providing a rich ground-truth for future multimodal research.
- We propose a methodology that automatically detects and describes three key categories of hallucinations. Our pipeline surpasses existing Vision-Language Model (VLM) baselines by providing granular, textual explanations of errors rather than isolated metrics.
- We define a formal taxonomy of hallucinations specific to the recontextualization task, offering a framework to better diagnose model reliability for sensitive use cases such as advertising and digital content creation.

2 Related Work

Hallucination detection in generative models has been approached from multiple perspectives, ranging from general, model-agnostic methods to task-specific techniques. In this section, we review methods that rely only on generated outputs, methods analyzing model behavior during generation, approaches based on input-output text–image alignment, and finally, methods specifically targeting hallucinations in image recontextualization.

Model agnostic hallucination detection Some approaches detect hallucinations using only the generated outputs. I-HallA [14] applies GPT-4o-based visual question answering to verify the factual consistency of generated outputs and releases a benchmark with textbook-derived prompts, hallucinated images, and human-validated QA pairs. WISE [17] provides a benchmark for real-world knowledge evaluation and a WiScore metric that measures semantic consistency and realism beyond text–image matching. LEGION [7] combines a synthetic dataset, SynthScars, with a framework that detects pixel-level artifacts, generates explanations, and guides image refinement. The authors in [5] use knowledge graphs to compare model outputs with ground-truth data, providing interpretable explanations of hallucinations in text generation.

Inference time hallucination detection Some methods detect hallucinations by analyzing model behavior during generation. For diffusion models [6, 25], the authors in [1] identify out-of-distribution samples caused by smooth approximations over discontinuous data manifolds and propose a trajectory-variance metric to detect hallucinations. Building on this, [27] uses generation-time adaptive sharpening along artifact-prone directions to prevent hallucinations while preserving valid interpolations. ESIDE [31] analyzes the intermediate timesteps of DDIM [26] inversion to detect artifacts in T2I and recontextualization models, providing explanations and benchmarks for evaluation. For LLMs, LapEigvals [2] examines attention graphs using spectral features to predict

hallucinations, while MB-ICL [28] selects in-context learning examples based on latent manifolds to improve the detection of factual inconsistencies across tasks.

Hallucination detection in text–image alignment For text-to-image and image captioning models, hallucination detection focuses on identifying inconsistencies between text and images. To measure text–image alignment, POPE [13] uses Yes/No questions derived from generated captions and images from the MSCOCO dataset [15]. CHAIR [21] measures the proportion of hallucinated objects among all objects mentioned in the text description. AMBER [29] improves on CHAIR by evaluating not only the existence but also the attributes and relationships between the objects. LURE [33] and Woodpecker [32] detect and correct hallucinations post-hoc, with LURE using co-occurrence patterns and uncertainty, and Woodpecker validating visual claims in multiple stages by first extracting key objects from the image and then querying a VLM with increasingly specific questions about each object. PA-ICVL [8] addresses pose-related and structural hallucinations in non-photorealistic output. The authors in [18] use knowledge-based question answering on scene graphs, while REVEALER [23] applies reinforcement learning and structured reasoning for element-level evaluation. The most prominent datasets for the validation of the above methods are GenAI-Bench [12], which provides large-scale human evaluation with VQA-based scoring, and AlignBench [22], which offers fully annotated image–caption pairs for detailed alignment assessment.

Image recontextualization hallucination detection Recent work has extended hallucination detection to image recontextualization and other multi-domain conditional generation tasks. VI-SCORE [9] introduces an instruction-guided, training-free metric that leverages multimodal LLMs to provide a task-aware, explainable evaluation with rationales in natural language. CIGEVAL [30] proposes an agentic evaluation framework that uses reasoning-based multimodal models to construct a dynamic, task-specific pipeline without any human-designed alignment or pipeline structure. ImagenHub [10] provides a unified library, dataset, and evaluation framework across multiple generation tasks, standardizing inference and human evaluation to measure semantic consistency, perceptual quality, and hallucinations in various models.

2.1 Gaps in Current Research

Despite growing interest in hallucination detection, most methods focus on text–image alignment, and only a few recent approaches address multimodal recontextualization. However, these methods [9, 30] typically quantify realism and alignment using simple scores, such as 0–10, and provide only unstructured textual descriptions of hallucinations. In contrast, our work introduces a detailed taxonomy of hallucinations and produces structured outputs that explicitly follow this taxonomy. Moreover, while there is a large existing benchmark [10] for recontextualization, it is based on automatic annotations. Our dataset is smaller but manually annotated, ensuring higher-quality labels that follow the defined taxonomy and support more precise evaluation.



(a) Reference image of object 1.



(b) Reference image of object 2.



(c) Background image.



(d) Generated image.

A photorealistic view of a spacious, modern dining room features dark green walls above white wainscoting, with three large windows centered on the far wall, letting in natural light; two woven rattan pendant lights hang from the ceiling. A three-seater brown leather sofa, detailed with button tufting, an open book on its seat, and a plaid throw blanket draped over its left arm, is placed centrally against the far wall beneath the windows. In the midground, to the left of the sofa, a black wooden armchair with a light grey cushion is angled slightly towards the sofa. Both pieces of furniture are realistically scaled and illuminated by the natural light from the windows, casting subtle shadows towards the viewer on the wooden floor, maintaining the original room's perspective and color harmony. No added text, no watermarks, no borders or frames, no unrelated objects.

Figure 1: Exemplary sample from the VIGIL Benchmark Dataset. Each sample includes: reference images for object 1 (a) and object 2 (b), the target background image (c), the final generated image (d), and the corresponding textual recontextualization prompt used for generation.

3 Dataset

To address the lack of benchmarks in the field of multimodal recontextualization, we constructed a dataset of 1,269 samples with five semantic categories: clothing, furniture, cosmetics, electronics, and cars. These domains were selected to mirror real-world applications in marketing and visually guided product design. A detailed breakdown is provided in Table 1. Each dataset entry consists of a background image, reference images for one or two objects, the resulting recontextualized image, and the textual prompt. Furthermore, each example includes JSON-formatted metadata containing assigned hallucination classes and explanatory rationales (see Figures 1, 2 for visual examples).

The dataset comprises 1,024 images containing hallucinations (80.7%) and 245 clean reference samples (19.3%). As a single image may exhibit multiple hallucinations, our taxonomic annotation yields 574 object errors, 402 spatial and instructional errors, 330 physical integration errors, 127 background errors, and 69 object omission errors.

Table 1: VIGIL Benchmark Dataset composition by category.

Category	Number of Samples
Clothing	497
Furniture	105
Cosmetics	223
Electronics	264
Cars	180

3.1 Data Preparation

Prompts for the recontextualization task were automatically synthesized using Gemini 2.5 Flash. We provided the model with a system prompt-constructed in accordance with the official Gemini guidelines, together with a set of reference images. The resulting prompts were manually inspected to verify their consistency with the input images and to ensure that no mismatches or semantic differences were introduced during the automatic generation process. The resulting instructions with images were then passed to Gemini 2.5 Flash Image to produce the final outputs. The hallucination classification and explanatory descriptions were performed entirely manually, without any involvement of language models during labeling.

3.2 Description of Data Source

All background and object images employed in this publication were acquired from publicly available online resources. In particular, for the clothing category, we used data from the Dress Code dataset [16]. For other categories, we curated a diverse collection of high-resolution images from Kaggle and Unsplash (electronics category), Douglas and Unsplash (cosmetics category), and via targeted web crawling for the furniture and cars categories.

3.3 Taxonomy of Hallucination Types

To systematically assess hallucinations produced by generative recontextualization models, we introduce a refined taxonomy that decomposes visual and structural inconsistencies into five distinct and non-overlapping categories. Each category isolates a specific

```

"hallucination": {
  "objects": "Object mutation: The chair has been
    modified into a rocking chair.",
  "background": "",
  "position_logic": "Misplacement: The couch is
    not positioned against the wall.",
  "physical": "",
  "object_omission": ""
}

```

Figure 2: JSON with assigned hallucination class(es) and descriptions from exemplary sample from the VIGIL Benchmark Dataset.

failure mode related to object appearance, background preservation, spatial reasoning, physical integration, or object presence (see Figure 3). Our approach focuses on distinguishing between localized artifacts and broader structural inconsistencies within the scene.

3.3.1 Object Visual Fidelity.

This category captures hallucinations related exclusively to the visual appearance of the objects instructed to be inserted into the scene. The evaluation focuses on whether its identity matches the reference. Object Visual Fidelity captures deviations in texture, material, color, and geometric structure. Two subtypes are distinguished: Object Mutation and Reference Bleeding (where visual traits from one reference object leak into another).

3.3.2 Background Fidelity.

Background Fidelity isolates hallucinations affecting the surrounding environment rather than the inserted objects. This includes all contextual elements that are expected to remain unchanged, such as walls, floors, windows, lighting, and preexisting furniture. Violations occur when the background is altered, simplified, or replaced. The identified subtypes are: Background Mutation and Context Swap.

3.3.3 Spatial & Instructional Fidelity.

This category captures failures related to spatial reasoning and compliance with high-level editing instructions. It concerns whether objects are placed in the correct locations, whether replacement or removal instructions are executed properly, and whether additional unintended objects are introduced. Appearance-related errors are excluded and handled by Object Visual Fidelity. The subtypes include Misplacement, Replacement Failure, and Unwanted Object Fabrication.

3.3.4 Physical & Integration Fidelity.

This category evaluates whether the inserted objects are coherently integrated into the physical and visual structure of the scene. This category captures violations of real-world consistency, including lighting, shadows, perspective, scale, and low-level rendering quality. The following subtypes are considered: Lighting and Shadow Incoherence, Perspective and Scale Issues, and Artifacts and Deformations.

3.3.5 Object Omission.

Object Omission refers to hallucinations in which the model fails

to generate one or more objects that are explicitly required by the input instructions. Unlike other categories, this failure mode is defined by the complete absence of an expected object.

4 Methodology

In this section, we describe the VIGIL pipeline methodology for hallucination detection in recontextualization tasks. To our knowledge, this is the first method specifically designed to focus on fine-grained hallucination detection, where multimodal consistency is crucial. The workflow, illustrated in Figure 4, decomposes verification into object-level fidelity and background consistency.

4.1 Object Extraction and Segmentation

The process begins by identifying the entities that must be preserved. We utilize Qwen3-VL-8B-Instruct to parse the recontextualization prompt, extracting the primary physical subjects. Once identified, we employ the Segment Anything Model 3 (SAM 3) to locate and mask these entities in both the reference and generated images (Segmented objects, Figure 4). This provides the spatial coordinates and masks necessary for comparative analysis.

4.2 Object Fidelity Verification

For each segmented object, we generate high-dimensional embeddings using DINO v3-ViT-B/16. To determine correspondences between reference and generated objects, we compute a cosine similarity matrix and apply the Linear Sum Assignment method to solve the bipartite matching problem (Object fidelity verification, Figure 4). The set of candidate pairs is restricted by semantic consistency; only pairs sharing the same class label, as assigned by SAM3, are considered potential matches.

A pair is considered a valid match only if it satisfies the condition $S_{cos} > \tau$. If a reference object fails to find a valid match, it is flagged as an *object omission* hallucination. Validated pairs are then passed back to the VLM (Qwen3-VL-8B-Instruct), which performs visual reasoning to detect *object mutations* or *reference bleeding* by comparing the segmented crops.

4.3 Background Fidelity Verification

To evaluate environmental integrity, we isolate the background by masking out all pixels belonging to the identified objects (Background fidelity verification, Figure 4). To ensure that the background evaluation is not biased by object-related artifacts, such as contact shadows and reflections, we extend the mask by a margin. The margin is calculated relative to the object's bounding box dimensions, ensuring that the exclusion zone adaptively scales to capture the peripheral influence of objects, regardless of their size. We employ two complementary methodologies.

- **Direct Comparative Analysis:** The VLM analyzes the masked reference and generated images to identify structural discrepancies or "context swaps."
- **Difference-Guided Localization:** We compute the absolute pixel-wise difference between the masked backgrounds to identify regions of high variance. Bounding boxes are drawn around these areas (Optional ROI localization, Figure 4), guiding the VLM to perform a targeted assessment of potential background hallucinations.

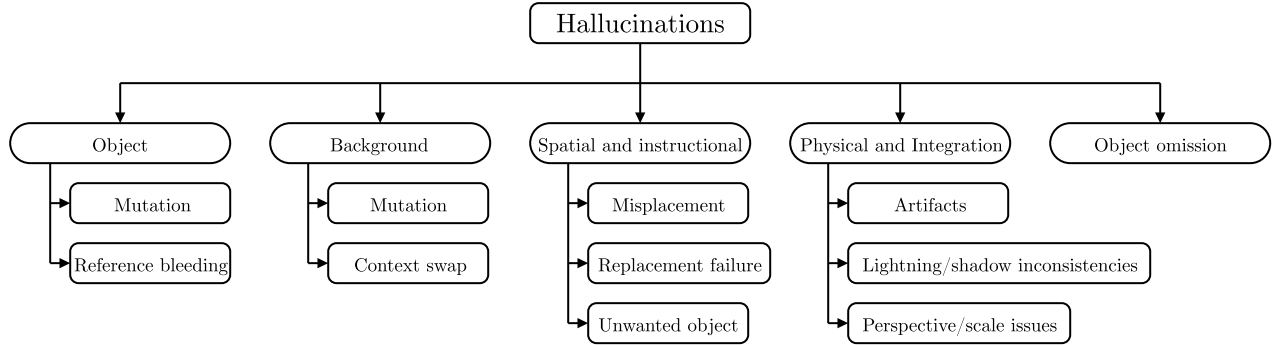


Figure 3: Overview of the taxonomy of hallucination types in VIGIL Benchmark Dataset.

In both methods, the model is instructed to distinguish between major structural errors and minor, natural modifications-such as contact shadows or subtle lighting adjustments-required for realistic object integration.

5 Experiments & Results

To evaluate the effectiveness of our proposed pipeline, we benchmarked its performance against the ground-truth annotations provided in our dataset. The evaluation focuses on the system's ability to accurately identify and categorize hallucinations in the recontextualized outputs.

To provide a comprehensive comparison, we also evaluated the performance of three commonly used vision-language models (VLMs) acting as standalone hallucination detectors: Gemini 2.5 Flash, Qwen3-VL-8B-Instruct, and Gemma 3 27B IT. We selected Qwen3-VL-8B-Instruct and Gemma 3 27B IT as they are the largest models in their respective families that can be run on a single GPU in our setup, with Qwen being used in our pipeline to assess its standalone performance. A direct comparison with methods such as [9] and [30] is not possible due to differences in output structure and task formulation.

For each baseline model, we followed a rigorous prompting protocol to ensure a fair comparison.

- **Prompt Optimization** - The models were queried using instructions tailored to their specific prompting guidelines to maximize their reasoning capabilities. We provide the example for the Gemini 2.5 Flash baseline prompt in Appendix B.
- **Definition of Hallucinations** - We provided the models with the exact taxonomy of hallucinations used during our manual annotation process, including detailed descriptions of object distortions, missing entities, and background inconsistencies.
- **Zero-Shot Detection** - Each model was presented with the source images, the text prompt, and the generated output without any task-specific training or fine-tuning and was tasked with identifying all visible hallucinations.

The results of these models were then compared against our annotations to determine how our multi-stage pipeline performs relative to the "all-in-one" detection approach of multimodal models.

5.1 Evaluation Metrics

To assess the performance of our hallucination detection pipeline, we employ two distinct evaluation frameworks. The first is based on multi-label classification metrics for binary detection, and the second is LLM-as-a-Judge for semantic consistency.

5.1.1 Multi-label Classification Performance.

We treat the detection task as a multi-label classification problem across three primary categories: Object Hallucinations, Background Inconsistencies, and Object Omissions. The **F1-score** is calculated for each hallucination type to evaluate the accuracy and robustness of the detection. Finally, we report macro-averaged scores, as the dataset is imbalanced both in terms of error types (TN, TP, FP, FN) and object categories (e.g., furniture, cars). Macro-averaging allows for a more balanced evaluation across categories.

5.1.2 LLM-as-a-Judge Semantic Evaluation.

Standard binary matching fails to capture the semantic nuance of natural language descriptions, particularly when multiple distinct hallucinations may be present within a single image. To address this, we employ Gemini 2.5 Flash as a semantic judge operating at a granular defect level. Instead of classifying the overall text alignment, the judge compares the set of hallucinations described by the pipeline against the human ground truth to quantify specific error instances. For each pair of descriptions, the model calculates **True Positives (TP)**, representing specific defects semantically present in both texts; **False Positives (FP)**, representing defects hallucinated by the pipeline but absent in the annotations; and **False Negatives (FN)**, representing ground-truth defects missed by the pipeline. These defect-level counts are subsequently used to compute F1-scores, ensuring that our metric reflects the system's ability to correctly identify and isolate individual visual anomalies.

5.2 Results

We calibrated our pipeline by varying three key parameters. We varied the cosine similarity threshold for object matching ($\tau \in$

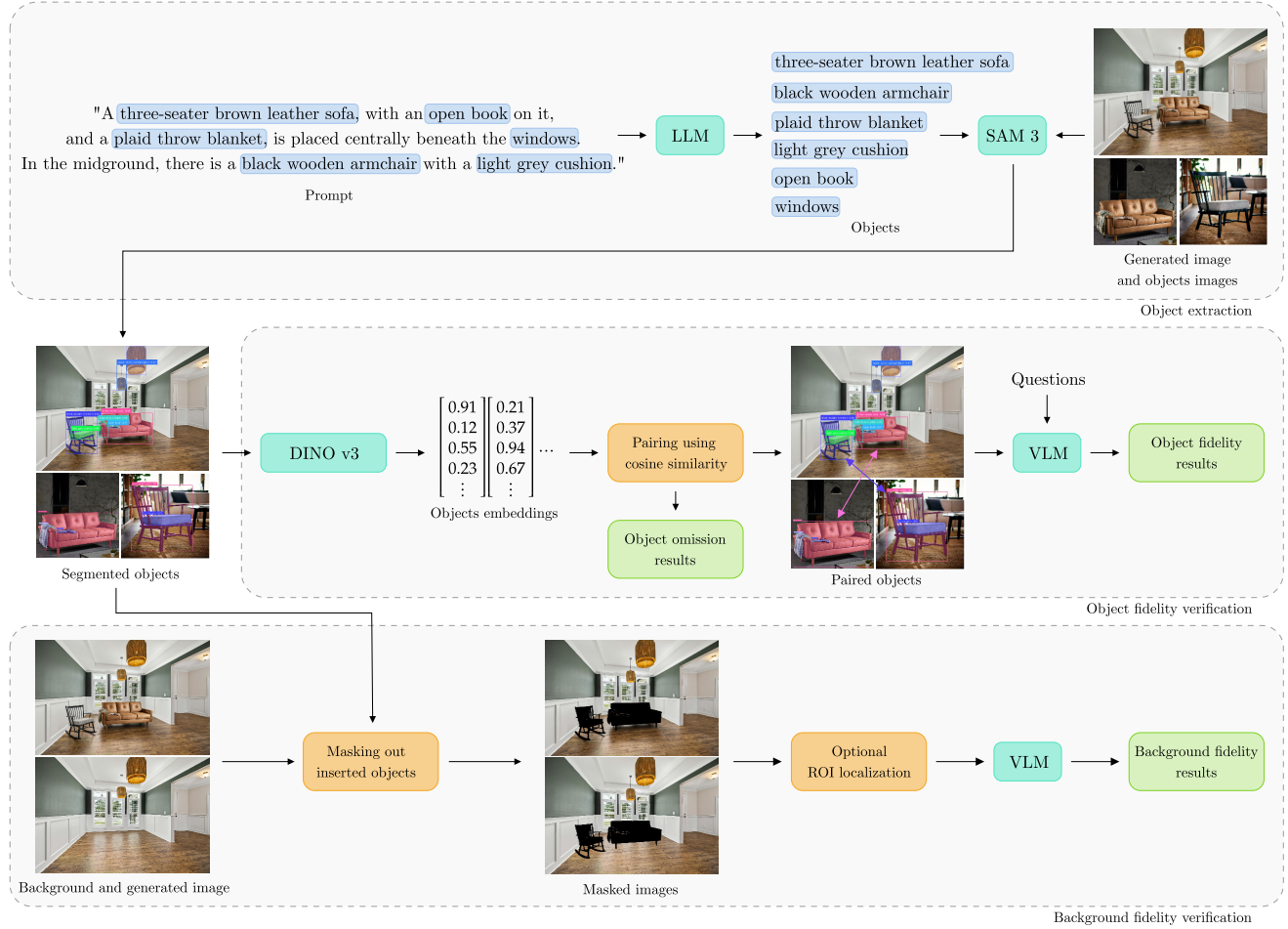


Figure 4: Overview of the pipeline. The framework consists of three modular stages: (1) **Object Extraction:** LLM-based entity parsing followed by SAM 3 segmentation. (2) **Object Fidelity Verification:** DINO v3 embedding generation and bipartite matching via cosine similarity to detect mutations or omissions. (3) **Background Fidelity Verification:** VLM-based comparison of masked images, enhanced by optional ROI localization of pixel-level variances to identify environmental hallucinations.

$\{0.1, 0.2, \dots, 0.8\}$), the spatial margin applied during object cropping ($\delta \in \{0.0, 0.1, 0.2\}$), and the inclusion of difference-based ROI bounding boxes for background verification.

The calibration was performed across our categories: cars, clothing, cosmetics, furniture, and electronics. To ensure robustness, we followed a leave-one-category-out strategy. For each split, we conducted a grid search on four categories and selected the best parameter set based on the Macro F1-score for the multi-label classification task. This selected configuration was then evaluated on the remaining category. We repeated this procedure for all possible 4+1 splits. We provide the detailed results in Appendix A.

The results are summarized in Table 2. We observe that in three categories, our method significantly outperforms all baselines, including Gemini 2.5 Flash.

We further analyzed our method using the LLM-as-a-Judge evaluation. In this setting, we considered only the parameter configurations previously selected as optimal for each category based on the

multi-label classification results, which account for all error types, including true negatives. As shown in Table 3, our method achieves the best performance for the clothing and cosmetics categories for LLM-as-a-Judge evaluation, which together comprise more than half of the VIGIL benchmark dataset. Moreover, across all categories, our approach outperforms both Qwen-3-VL-8B-Instruct and Gemma 3 27B IT baselines.

Outperforming Qwen is particularly important, as this model is used multiple times within our VIGIL pipeline. The results show that when Qwen3-VL-8B-Instruct is applied in a decomposed setting, where it is assigned a more focused and limited subtask, it achieves stronger performance than when used as a standalone baseline.

In general, the relatively low F1-scores reported in Table 3 result from the difficulty VLMs have in detecting subtle errors. The errors themselves are, however, accurately counted by the LLM-as-a-judge framework, as it relies on a strong judging model (Gemini 2.5 Flash).

Table 2: Macro F1-Score for Multi-label Classification for the best set of parameters on test category (the remaining categories were assigned to the calibration set for the pipeline).

Method	Clothing	Furniture	Cosmetics	Electronics	Cars
Gemini 2.5 Flash	0.3649	0.3058	0.1441	0.2404	0.3962
Qwen3-VL-8B-Instruct	0.2852	0.3357	0.1486	0.2047	0.2421
Gemma 3 27B IT	0.2534	0.3487	0.1745	0.2227	0.3611
VIGIL (ours)	0.5029	0.3841	0.2275	0.1636	0.3306

Table 3: Macro F1-Score for LLM-as-a-Judge evaluation for the best set of parameters on test category (the remaining categories were assigned to the calibration set for the pipeline).

Method	Clothing	Furniture	Cosmetics	Electronics	Cars
Gemini 2.5 Flash	0.2251	0.1702	0.0627	0.1216	0.1907
Qwen3-VL-8B-Instruct	0.1136	0.1103	0.0237	0.0255	0.0224
Gemma 3 27B IT	0.0861	0.0819	0.0025	0.0146	0.1040
VIGIL (ours)	0.3414	0.1422	0.1042	0.0354	0.1863

6 Potential Applications

The VIGIL framework offers significant utility across several domains. In digital marketing, it ensures brand integrity by verifying that product attributes remain constant during automated scene generation. In e-commerce, our pipeline facilitates high-fidelity virtual try-on systems by flagging garment mutations. Furthermore, the dataset serves as a rigorous diagnostic tool for model developers, allowing them to identify whether architectural weaknesses lie in spatial reasoning or low-level feature preservation.

7 Discussion and Limitations

While the VIGIL pipeline demonstrates superior performance in category-specific F1-scores, particularly in the Clothing and Cosmetics part of the dataset, several limitations warrant consideration. The nature of our architecture, involving SAM 3, DINO v3, and Qwen3-VL-8B-Instruct, introduces significant computational overhead. Furthermore, model scaling is currently bounded by hardware availability; while larger variants could potentially improve reasoning, we utilize smaller model iterations to ensure compatibility with the memory constraints of a single A100 40 GB GPU. Temporal and technical factors also impact our dataset quality. The initial image set was generated prior to the availability of Gemini 3 Pro Image, resulting in lower native resolutions than current state-of-the-art outputs. This leads to a scale discrepancy during evaluation: when a generated object occupies only a small percentage of the frame compared to a reference image in which it occupies most of the pixels, the model essentially compares low-resolution artifacts against high-fidelity data. In such cases, the system lacks sufficient visual information for an accurate assessment. Additionally, our evaluation framework faces specific challenges regarding semantic accuracy. If a generated object is not correctly paired or aligned with its reference counterpart, background evaluation metrics become distorted and unreliable. There remains a risk of the model confusing similar objects—such as different products within a single cosmetics line where visual features are nearly identical. Finally,

our LLM-as-a-Judge approach, while more nuanced than binary metrics, may still inherit latent biases from the underlying evaluator model.

Future iterations of the methodology should prioritize the development of a dedicated evaluation framework for spatial relations, integrating advanced depth estimation to accurately verify relations such as *in front of*, *behind*, *leaning against*. Beyond this, it should also incorporate a physical consistency evaluation to determine the structural plausibility of generated scenes, ensuring that objects obey gravity and environmental logic.

8 Conclusion

In this work, we introduced VIGIL, a comprehensive framework designed to address the critical challenge of hallucination detection in multimodal image recontextualization. By establishing a fine-grained taxonomy and curating a manually annotated benchmark dataset of 1,269 samples, we have moved beyond generic alignment scores to a structured diagnostic approach that isolates specific failure modes, such as object mutations and background inconsistencies.

Our experimental results demonstrate that decomposing the detection process into specialized modules—specifically targeting object fidelity and background consistency—yields superior performance compared to monolithic state-of-the-art VLMs. The VIGIL pipeline showed particular strength in domains requiring high visual precision, such as clothing and cosmetics, validating the effectiveness of integrating discriminative models like DINO v3 with generative reasoners. This suggests that while general-purpose multimodal models are powerful, they benefit significantly from structured, multi-stage guidance when tasked with identifying subtle visual hallucinations.

As generative models become integral to high-stakes industries like e-commerce and digital advertising, the ability to automatically verify visual integrity is paramount. While our current approach effectively targets semantic and visual fidelity, future developments will focus on integrating geometric and physical reasoning to address spatial and structural hallucinations more robustly. We hope the VIGIL benchmark and methodology serve as a foundational resource for the research community, driving further advancements in the reliability and explainability of Large Multimodal Models.

9 Statements and Declarations

We gratefully acknowledge Polish high-performance computing infrastructure PLGrid (HPC Center: ACK Cyfronet AGH) for providing computer facilities and support within computational grant no. PLG/2025/018661.

References

- [1] Sumukh K Aithal, Pratyush Maini, Zachary Lipton, and J Zico Kolter. 2024. Understanding hallucinations in diffusion models through mode interpolation. *Advances in Neural Information Processing Systems* 37 (2024), 134614–134644.
- [2] Jakub Binkowski, Denis Janiak, Albert Sawczyn, Bogdan Gabrys, and Tomasz Jan Kajdanowicz. 2025. Hallucination detection in llms using spectral features of attention maps. In *Proceedings of the 2025 Conference on Empirical Methods in Natural Language Processing*. 24365–24396.
- [3] Nicolas Carion, Laura Gustafson, Yuan-Ting Hu, Shoubhik Debnath, Ronghang Hu, Didac Suris, Chaitanya Ryali, Kalyan Vasudev Alwala, Haitham Khedr, Andrew Huang, Jie Lei, Tengyu Ma, Baishan Guo, Arpit Kalla, Markus Marks, Joseph Greer, Meng Wang, Peize Sun, Roman Rädl, Triantafyllos Afouras, Effrosyni

Mavroudi, Katherine Xu, Tsung-Han Wu, Yu Zhou, Liliane Momeni, Rishi Hazra, Shuangrui Ding, Sagar Vaze, Francois Porcher, Feng Li, Siyuan Li, Aishwarya Kamath, Ho Kei Cheng, Piotr Dollár, Nikhila Ravi, Kate Saenko, Pengchuan Zhang, and Christoph Feichtenhofer. 2025. SAM 3: Segment Anything with Concepts. *arXiv:2511.16719 [cs.CV]* <https://arxiv.org/abs/2511.16719>

[4] Gemini Team, Google. 2025. Gemini: A Family of Highly Capable Multimodal Models. *arXiv:2312.11805 [cs.CL]* <https://arxiv.org/abs/2312.11805>

[5] Reilly Haskins and Benjamin Adams. 2025. Kea explain: Explanations of hallucinations using graph kernel analysis. *arXiv preprint arXiv:2507.03847* (2025).

[6] Jonathan Ho, Ajay Jain, and Pieter Abbeel. 2020. Denoising diffusion probabilistic models. *Advances in neural information processing systems* 33 (2020), 6840–6851.

[7] Hengrui Kang, Siwei Wen, Zichen Wen, Junyan Ye, Weijia Li, Peilin Feng, Baichuan Zhou, Bin Wang, Dahua Lin, Linfeng Zhang, et al. 2025. Legion: Learning to ground and explain for synthetic image detection. *arXiv preprint arXiv:2503.15264* (2025).

[8] Bumsoo Kim, Wonseop Shin, Kyuchul Lee, Yonghoon Jung, and Sanghyun Seo. 2025. Make VLM Recognize Visual Hallucination on Cartoon Character Image with Pose Information. In *2025 IEEE/CVF Winter Conference on Applications of Computer Vision (WACV)*. IEEE, 5398–5407.

[9] M Ku, D Jiang, C Wei, X Yue, and W Chen. 2023. Viescore: Towards explainable metrics for conditional image synthesis evaluation. *arXiv*.

[10] Max Ku, Tianle Li, Kai Zhang, Yujie Lu, Xingyu Fu, Wenwen Zhuang, and Wenhui Chen. 2023. Imagenhub: Standardizing the evaluation of conditional image generation models. *arXiv preprint arXiv:2310.01596* (2023).

[11] Black Forest Labs, Stephen Batifol, Andreas Blattmann, Frederic Boesel, Saksham Consul, Cyril Diagne, Tim Dockhorn, Jack English, Zion English, Patrick Esser, Sumith Kulal, Kyle Lacey, Yam Levi, Cheng Li, Dominik Lorenz, Jonas Müller, Dustin Podell, Robin Rombach, Harry Saini, Axel Sauer, and Luke Smith. 2025. FLUX.1 Kontext: Flow Matching for In-Context Image Generation and Editing in Latent Space. *arXiv:2506.15742 [cs.GR]* <https://arxiv.org/abs/2506.15742>

[12] Baiqi Li, Zhiqiu Lin, Deepak Pathak, Jiayao Li, Yixin Fei, Kewen Wu, Tiffany Ling, Xide Xia, Pengchuan Zhang, Graham Neubig, et al. 2024. Genai-bench: Evaluating and improving compositional text-to-visual generation. *arXiv preprint arXiv:2406.13743* (2024).

[13] Yifan Li, Yifan Du, Kun Zhou, Jinpeng Wang, Wayne Xin Zhao, and Ji-Rong Wen. 2023. Evaluating object hallucination in large vision-language models. *arXiv preprint arXiv:2305.10355* (2023).

[14] Youngsun Lim, Hojun Choi, and Hyunjung Shim. 2025. Evaluating Image Hallucination in Text-to-Image Generation with Question-Answering. In *Proceedings of the AAAI Conference on Artificial Intelligence*, Vol. 39. 26290–26298.

[15] Tsung-Yi Lin, Michael Maire, Serge Belongie, James Hays, Pietro Perona, Deva Ramanan, Piotr Dollár, and C Lawrence Zitnick. 2014. Microsoft coco: Common objects in context. In *European conference on computer vision*. Springer, 740–755.

[16] Davide Morelli, Matteo Fincato, Marcella Cornia, Federico Landi, Fabio Cesari, and Rita Cucchiara. 2022. Dress Code: High-Resolution Multi-Category Virtual Try-On. In *Proceedings of the European Conference on Computer Vision*.

[17] Yuwei Niu, Munan Ning, Mengren Zheng, Weiyang Jin, Bin Lin, Peng Jin, Jiaqi Liao, Chaoran Feng, Kunpeng Ning, Bin Zhu, et al. 2025. Wise: A world knowledge-informed semantic evaluation for text-to-image generation. *arXiv preprint arXiv:2503.07265* (2025).

[18] Ziyuan Qin, Dongjie Cheng, Haoyu Wang, Huahui Yi, Yuting Shao, Zhiyuan Fan, Kang Li, and Qicheng Lao. 2024. Evaluating Hallucination in Text-to-Image Diffusion Models with Scene-Graph based Question-Answering Agent. *arXiv preprint arXiv:2412.05722* (2024).

[19] Qwen Team. [n. d.]. Qwen3-VL Technical Report.

[20] Aditya Ramesh, Mikhail Pavlov, Gabriel Goh, Scott Gray, Chelsea Voss, Alec Radford, Mark Chen, and Ilya Sutskever. 2021. Zero-Shot Text-to-Image Generation. *arXiv:2102.12092 [cs.CV]* <https://arxiv.org/abs/2102.12092>

[21] Anna Rohrbach, Lisa Anne Hendricks, Kaylee Burns, Trevor Darrell, and Kate Saenko. 2018. Object hallucination in image captioning. *arXiv preprint arXiv:1809.02156* (2018).

[22] Kuniaki Saito, Risa Shinoda, Shohei Tanaka, Toshio Hirasawa, Fumio Okura, and Yoshitaka Ushiku. 2025. AlignBench: Benchmarking Fine-Grained Image-Text Alignment with Synthetic Image-Caption Pairs. *arXiv preprint arXiv:2511.20515* (2025).

[23] Fulin Shi, Wenyi Xiao, Bin Chen, Liang Din, and Leilei Gan. 2025. REVEALER: Reinforcement-Guided Visual Reasoning for Element-Level Text-Image Alignment Evaluation. *arXiv preprint arXiv:2512.23169* (2025).

[24] Oriane Siméoni, Huy V. Vo, Maximilian Seitzer, Federico Baldassarre, Maxime Oquab, Cijo Jose, Vasil Khalidov, Marc Szafraniec, Seungeun Yi, Michaël Ramamorjisoa, Francisco Massa, Daniel Haziza, Luca Wehrstedt, Jianyuan Wang, Timothée Darcret, Théo Moutakanni, Leonel Sentana, Claire Roberts, Andrea Vedaldi, Jamie Tolan, John Brandt, Camille Couprie, Julien Mairal, Hervé Jégou, Patrick Labatut, and Piotr Bojanowski. 2025. DINOv3. *arXiv:2508.10104 [cs.CV]* <https://arxiv.org/abs/2508.10104>

[25] Jascha Sohl-Dickstein, Eric Weiss, Niru Maheswaranathan, and Surya Ganguli. 2015. Deep unsupervised learning using nonequilibrium thermodynamics. In *International conference on machine learning*. pmlr, 2256–2265.

[26] Jiaming Song, Chenlin Meng, and Stefano Ermon. 2020. Denoising diffusion implicit models. *arXiv preprint arXiv:2010.02502* (2020).

[27] Kostas Triaridis, Alexandros Graikos, Aggelina Chatziagapi, Grigorios G Chrysos, and Dimitris Samaras. 2025. Mitigating Diffusion Model Hallucinations with Dynamic Guidance. *arXiv preprint arXiv:2510.05356* (2025).

[28] Bodla Krishna Vamshi, Rohan Bhatnagar, and Haizhao Yang. 2026. Manifold-based Sampling for In-Context Hallucination Detection in Large Language Models. *arXiv preprint arXiv:2601.06196* (2026).

[29] Junyang Wang, Yuhang Wang, Guohai Xu, Jing Zhang, Yukai Gu, Haitao Jia, Jiaqi Wang, Haiyang Xu, Ming Yan, Ji Zhang, et al. 2023. Amber: An llm-free multi-dimensional benchmark for mllms hallucination evaluation. *arXiv preprint arXiv:2311.07397* (2023).

[30] Jifang Wang, Yangxue Yangxue, Longyue Wang, Zhenran Xu, Yiyu Wang, Yaowei Wang, Weihua Luo, Kaifu Zhang, Baotian Hu, and Min Zhang. 2025. A unified agentic framework for evaluating conditional image generation. In *Proceedings of the 63rd Annual Meeting of the Association for Computational Linguistics (Volume 1: Long Papers)*. 12626–12646.

[31] Yixin Wu, Feiran Zhang, Tianyuan Shi, Ruicheng Yin, Zhenghua Wang, Zhenliang Gan, Xiaohua Wang, Changze Lv, Xiaoqing Zheng, and Xuanjing Huang. 2025. Explainable Synthetic Image Detection through Diffusion Timestep Ensemble. *arXiv preprint arXiv:2503.06201* (2025).

[32] Shukang Yin, Chaoyou Fu, Sirui Zhao, Tong Xu, Hao Wang, Dianbo Sui, Yunhang Shen, Ke Li, Xing Sun, and Enhong Chen. 2024. Woodpecker: Hallucination correction for multimodal large language models. *Science China Information Sciences* 67, 12 (2024), 220105.

[33] Yiyang Zhou, Chenhang Cui, Jaehong Yoon, Linjun Zhang, Zhun Deng, Chelsea Finn, Mohit Bansal, and Huaxiu Yao. 2023. Analyzing and mitigating object hallucination in large vision-language models. *arXiv preprint arXiv:2310.00754* (2023).

A Grid search results

Table 4 presents the results of a comprehensive grid search conducted to optimize the VIGIL pipeline’s hyperparameters across different semantic categories. We evaluated the impact of the cosine similarity matching threshold ($\tau \in \{0.1, 0.2, \dots, 0.8\}$), the spatial margin applied during object cropping ($\delta \in \{0.0, 0.1, 0.2\}$), and the inclusion of difference-based ROI bounding boxes (*Boxes*) for background verification.

The configurations yielding the highest F1 scores for each category (highlighted in bold) were selected for final evaluation on the test split. It is worth noting that the optimal hyperparameter settings are consistent across diverse semantic tasks, typically favoring a low threshold ($\tau = 0.1$) and a wider spatial margin ($\delta = 0.2$). This uniformity demonstrates that the VIGIL method is robust and maintains high performance without the need for exhaustive per-category manual tuning.

Table 4: Experiment Results: Binary Classification F1 Scores

Threshold	Margin	Boxes	Binary classification F1 score - all classes except				
			Cars	Clothes	Cosmetics	Electronics	Furniture
0.1	0.0	False	0.3261	0.2806	0.3426	0.3604	0.3132
0.1	0.0	True	0.3137	0.2707	0.3369	0.3542	0.3041
0.1	0.1	False	0.3215	0.2811	0.3424	0.3653	0.3113
0.1	0.1	True	0.3237	0.2780	0.3488	0.3607	0.3116
0.1	0.2	False	0.3283	0.2853	0.3453	0.3701	0.3149
0.1	0.2	True	0.3223	0.2829	0.3461	0.3606	0.3094
0.2	0.0	False	0.3238	0.2773	0.3419	0.3613	0.3078
0.2	0.0	True	0.3098	0.2646	0.3350	0.3540	0.2985
0.2	0.1	False	0.3151	0.2749	0.3384	0.3637	0.3064
0.2	0.1	True	0.3201	0.2738	0.3465	0.3616	0.3022
0.2	0.2	False	0.3193	0.2752	0.3376	0.3653	0.3074
0.2	0.2	True	0.3178	0.2778	0.3433	0.3606	0.3020
0.3	0.0	False	0.3133	0.2616	0.3276	0.3529	0.2964
0.3	0.0	True	0.3031	0.2527	0.3241	0.3475	0.2906
0.3	0.1	False	0.3065	0.2574	0.3245	0.3525	0.2944
0.3	0.1	True	0.3106	0.2582	0.3319	0.3532	0.2913
0.3	0.2	False	0.3150	0.2648	0.3302	0.3623	0.2986
0.3	0.2	True	0.2431	0.1951	0.2678	0.2749	0.2267
0.4	0.0	False	0.3160	0.2616	0.3246	0.3546	0.2891
0.4	0.0	True	0.2408	0.1960	0.2749	0.2823	0.2267
0.4	0.1	False	0.3099	0.2555	0.3201	0.3535	0.2865
0.4	0.1	True	0.3123	0.2572	0.3290	0.3518	0.2866
0.4	0.2	False	0.3171	0.2625	0.3265	0.3618	0.2943
0.4	0.2	True	0.3086	0.2572	0.3246	0.3507	0.2844
0.5	0.0	False	0.3034	0.2555	0.3080	0.3424	0.2762
0.5	0.0	True	0.2883	0.2381	0.3019	0.3310	0.2669
0.5	0.1	False	0.3002	0.2553	0.3091	0.3455	0.2790
0.5	0.1	True	0.2960	0.2440	0.3087	0.3371	0.2713
0.5	0.2	False	0.3062	0.2580	0.3124	0.3496	0.2833
0.5	0.2	True	0.2959	0.2484	0.3083	0.3382	0.2708
0.6	0.0	False	0.2000	0.1590	0.2221	0.2317	0.1844
0.6	0.0	True	0.2533	0.2184	0.2694	0.2953	0.2376
0.6	0.1	False	0.2693	0.2376	0.2773	0.3098	0.2518
0.6	0.1	True	0.2577	0.2210	0.2724	0.2985	0.2390
0.6	0.2	False	0.2728	0.2379	0.2756	0.3127	0.2534
0.6	0.2	True	0.2567	0.2230	0.2704	0.2972	0.2399
0.7	0.0	False	0.2239	0.1993	0.2222	0.2579	0.2188
0.7	0.0	True	0.2114	0.1874	0.2190	0.2483	0.2094
0.7	0.1	False	0.2262	0.2058	0.2260	0.2634	0.2238
0.7	0.1	True	0.2169	0.1906	0.2241	0.2520	0.2118
0.7	0.2	False	0.1681	0.1434	0.1887	0.1959	0.1743
0.7	0.2	True	0.1624	0.1433	0.1790	0.1929	0.1596
0.8	0.0	False	0.1734	0.1671	0.1649	0.2082	0.1736
0.8	0.0	True	0.1621	0.1540	0.1630	0.1968	0.1659
0.8	0.1	False	0.1751	0.1704	0.1698	0.2110	0.1783
0.8	0.1	True	0.1630	0.1533	0.1633	0.1966	0.1653
0.8	0.2	False	0.1792	0.1728	0.1692	0.2137	0.1800
0.8	0.2	True	0.1651	0.1540	0.1629	0.1975	0.1658

B Exemplary prompt used for Gemini 2.5 Flash baseline

You are an image re-contextualization hallucination inspector. You will be given:

- An instruction prompt (what the generator was asked to do),
- A background image (background image),
- Reference object image(s) (one or two) - object 1 image, object 2 image,
- The generated image (generated image) - result of re-contextualization.

Your task: compare the generated image to the references and to the instruction, and produce THREE SHORT SEMANTIC DESCRIPTIONS (1-3 sentences each) answering the following categories. If no issues or hallucinations are detected in a category, return an empty string ("") for that category.

Categories:

1) objects: Object Visual Fidelity - texture/shape/color identity mismatches, mutations, identity loss, reference bleeding. Example: "Feature Mutation: sofa's color changed from dark green to black; Identity Loss: inserted cabinet is metallic vs wicker."

2) background: Background Fidelity - background mutations, background detail loss, context swap. Example: "Background Mutation: wall color changed; Context Swap: bedroom replaced by living room."

3) object omission: Object Omission - missing required objects from the instruction that should have been pasted from object image. Example: "Object Omission: green cabinet missing."

Instruction Prompt: {instruction prompt}

Analyze the provided images now.

The prompt follows multimodal design principles by assigning a specific role and breaking the task into three distinct categories: object fidelity, background fidelity, and objects omissions. This structure directs the model's attention to specific visual elements and provides clear semantic definitions for errors, ensuring consistent evaluation without the need for visual examples.